Progress in Automatic Aerial Triangulation

TONI SCHENK, Ohio State University, Columbus

ABSTRACT

This paper summarizes the most important conclusions that can be drawn from recent developments in automatic aerial triangulation. The focus of the paper is on a shift from points to linear and areal features. After motivating this shift, the paper deals extensively with the use of control features to recover the exterior orientation parameters. Two different approaches are presented, namely an image point to control feature relationship, and an image feature to control feature relationship. The latter relationship requires fitting the appropriate feature through data points. The paper continues with an account of remaining problems and concludes with suggested future research and directions of automatic aerial triangulation.

1 Introduction

The transition from analytical plotters to digital photogrammetric workstations also had a significant impact on aerial triangulation. It lead to what may be called *interactive aerial triangulation*. Most vendors of digital photogrammetric workstations offer software tools that greatly assist the operator in conducting aerial triangulation. Interactive methods offer the advantage of having a human operator in the loop who can intervene if something goes wrong or makes decisions upon system requests. In that way, automation of aerial triangulation can be gradually introduced.

Automatic aerial triangulation sets out to perform all the necessary processes automatically, without much assistance from a human operator. The ultimate goal would be to have a black box system that does not need any intervention at all. There is no sharp boundary between interactive and automatic aerial triangulation. One may argue that a sophisticated interactive system may be superior to an inflexible, non-robust automatic aerial triangulation system.

Remarkable progress has been achieved in automatic aerial triangulation during the past few years. Undoubtedly, the single most important activity was the OEEPE test on integrated sensor orientation, *Heipke et al.* (2002). At the occasion of the OEEPE workshop in Hannover, Sept. 17-18, 2001, several researchers presented their findings and shed light on some of the pending issues.

From these OEEPE related activities and recent developments we comment on a few points. Commercially available automatic aerial triangulation programs have reached a high level of performance and flexibility allowing smooth and efficient processing of large blocks. The capability of programs developed at research institutions are perhaps less well advertised and therefore less well known. They usually sacrifice robustness, support, ease of use, and documentation for a higher level of sophistication and flexibility in the mathematical models.

We can also conclude that there is a much better understanding of the question direct vs. indirect orientation, about the intricate relationship of sensor calibration, and the effect of interior and exterior orientation. Perhaps less well known is the accuracy aspect of computed block points from direct or indirect orientation. *Habib and Schenk* (2001) present a detailed analysis which shows that the accuracy of block points is inferior in direct orientation even if the orientation parameters have small errors. This is a consequence of a different error propagation between the two methods.

Yet another conclusion is that automatic aerial triangulation is entirely point based. Most authors seem to make a claim of using features but a closer look reveals that points are meant. We take the point/feature issue as the central part of this paper. The next section provides a motivation for using features and suggests a closer integration of automatic aerial triangulation with other photogrammetric procedures. Section 3 is devoted to the use of control features, such as straight lines, analytical curves, free-form curves, planar surfaces, and free-form surfaces. The presented mathematical models are based on an image point to control feature relationship, or, if possible, an image feature to control feature relationship. Section 4 lists some of the most important problems to be solved, including tie features, curve fitting, and multisensor automatic aerial triangulation. The paper concludes by summarizing the most pertinent points discussed and suggests future developments.

2 Feature-Based Aerial Triangulation

As noted in the previous section, automatic aerial triangulation is predominantly point-based, presumably because it is more challenging to extract linear and areal features and to use them in the mathematical models of automatic aerial triangulation. Despite these difficulties, we strongly argue for moving from a point-based to feature-based photogrammetry, see also *Schenk* (2002).

In automatic photogrammetry computer operators assume the role of human operators. However, computer operators are far inferior with regards to selecting meaningful points in aerial triangulation. Although points can be extracted easily with an interest operator, they carry almost no semantic information about a scene. In contrast, linear and areal features may be related to objects. For example, an edge in the image may correspond to an object boundary, and a region to physical surface. In view of object extraction, features are clearly more meaningful primitives than points.

Now the critical reader may raise the question why we should be concerned of integrating automatic aerial triangulation with other applications that need features? To answer the question we refer to Fig. 1. The left side shows the traditional process of aerial triangulation and the relationship to subsequent processes. Aerial triangulation is a self-contained process with the goal to determine the exterior orientation of all images involved in a project. This is to narrow a view, however, because aerial triangulation also produces valuable information about the object space, namely all the tie points. The object space information is hardly used, however, except perhaps if stereomodels are being set up and tie points are used to orient the models (as an alternative to use the exterior orientation parameters) in order to manually minimize the $y-$parallaxes.

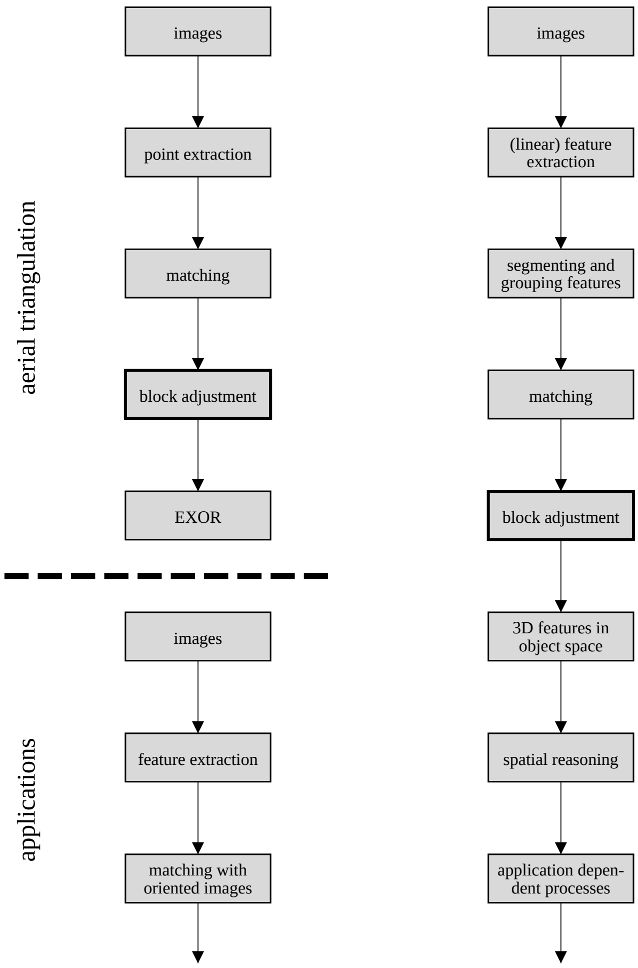

Figure 1: The left hand side depicts a blockdiagram of aerial triangulation and photogrammetric applications. Note the clear separation of the processes. The right hand side suggests a closer integration.

The right hand side of Fig. 1 suggests a closer integration of aerial triangulation with subsequent photogrammetric processes, such as DEM/DTM generation or automated mapping. The differences to the traditional approach may appear subtle but are important. As argued in the previous section, the orientation should preferably be performed with the same features that are used in applications.

As the figure indicates, the raw extracted features are further processed. Segmentation for example, would extract straight lines and second order curves (curvi-linear segmentation). An example of a typical grouping process is finding straight lines that have a particular orientation with each other, e.g. parallel lines, or lines at right angles. These grouping processes are at the heart of perceptual organization that aims at finding structure in features. In object recognition, such structures can be compared with models of objects and if sufficient agreement between image structures and model is found, a hypothesis about the instance of an object can be generated.

The major advantage of incorporating more abstract features is two fold. For one, matching abstract features is a lot more robust than matching low level image primitives, although it is considerably more complex to implement it. Successfully matched structures, perhaps in multiple images, may assume the role of tie features and after automatic aerial triangulation, they are represented in object space, allowing scene interpretation in the 3D object space.

Surface reconstruction is a good example for tightly coupling automatic aerial triangulation with automatic DEM generation. In fact, there is no reason why sensor orientation and surface reconstruction must be completely separate processes.

3 Orientation with Control Features

In this section we will examine the use of known linear and areal features in object space, called control features, instead of control points. Linear features include straight lines, analytical curves (space curves), and free-form lines. Straight lines and to a lesser degree space curves may be known in object space in urban areas while free-form lines are more likely to occur in natural scenes, for example roads or other extended features stored in a GIS.

Control surfaces are increasingly available from LIDAR projects or in form of existing DEMs/ DTMs. If a control surface derived from LIDAR is used then orienting images with respect to this surface is an ideal registration or fusion of the two sensors.

We assume that some control features are imaged, at least partially and that this partial projection can be extracted, for example by an edge operator. In the following, we call this extracted feature *image feature*. The goal is to derive a relationship between control feature, image feature, and the orientation parameters, based on which a suitable target function can be designed for unbiased estimate of the orientation parameters.

There are two principally different ways to establish a relationship between image and control feature. The first approach takes a point of the image feature, for example an edge pixel, and minimizes the distance of the bundle ray and the control feature. This will lead to modified collinearity equations. In the second approach, the image feature is represented as an entity like the control feature. This entails fitting a straight line or a curve through instances of the image feature. Then, a relationship of entities is established that usually renders condition equations.

It is possible to combine both methods in an orientation problem to take advantage and avoid disadvantages that are associated to both methods.

3.1 Orientation with Straight Lines

3.1.1 Image Point to Control Line Relationship

To illustrate the case of using observed points on an image feature that corresponds to a 3D control feature, we use the example of straight lines. Suppose a known straight line in object space is partially imaged and detected by an edge operator, for example. As shown in Fig. 2(a), we can extend the standard collinearity model such that the bundle ray from the perspective center through an edge point intersects the control line. This situation can conveniently be expressed by the parametric representation of the control line because. That is, the unknown point of intersection is defined by line parameter t. Let points A and B define the control line. Then any point on this line is defined by

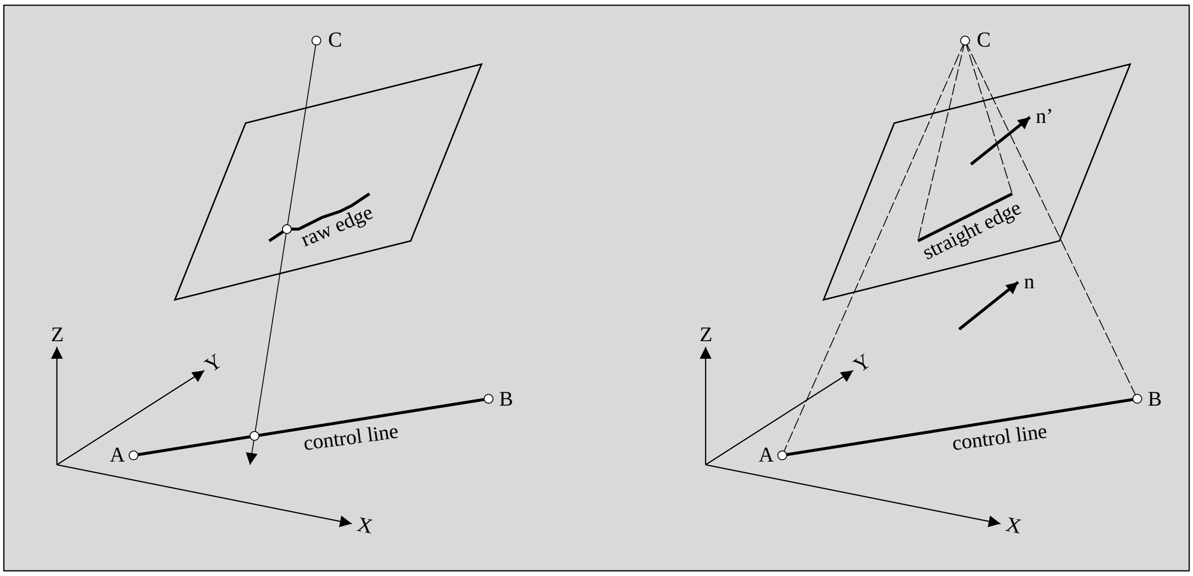

Figure 2: Illustration of edge point to control line relationship (left pane) and image line to control line relationship (right pane).

$$
\begin{aligned}
X &= X_A + t \cdot a \\
Y &= Y_A + t \cdot b \\
Z &= Z_A + t \cdot c
\end{aligned}
\tag{1}
$$

with a, b, c the components of the direction vector and t the line parameter.

Now, in the standard collinearity model we substitute object point P by above equation and obtain the extended model

$$
\begin{aligned}
x_p &= -f \frac{(X_A + t \cdot a - X_C)r_{11} + (Y_A + t \cdot b - Y_C)r_{12} + (Z_A + t \cdot c - Z_C)r_{13}}{(X_A + t \cdot a - X_C)r_{31} + (Y_A + t \cdot b - Y_C)r_{32} + (Z_A + t \cdot c - Z_C)r_{33}} \\
y_p &= -f \frac{(X_A + t \cdot a - X_C)r_{21} + (Y_A + t \cdot b - Y_C)r_{22} + (Z_A + t \cdot c - Z_C)r_{23}}{(X_A + t \cdot a - X_C)r_{31} + (Y_A + t \cdot b - Y_C)r_{32} + (Z_A + t \cdot c - Z_C)r_{33}}
\end{aligned}
\tag{2}
$$

with x_p, y_p an observed edge point, r_{ij} the elements of the orthogonal rotation matrix, and X_C, Y_C, Z_C the perspective center. The perspective center, the three attitude angles of the rotation matrix, and line parameter t are the 7 unknowns to be estimated for one image and one observed point. Considering the degree of freedom of two for straight lines, we can form another independent observation equation of the form 2. Not surprisingly, three non-collinear control lines are needed to determine the exterior orientation parameters. Observing more than 2 points on a edge does not contribute towards the reduction of the datum defect but increases the redundancy and thus positively influences the accuracy. Note that even if only one point per edge is used, the orientation can be solved, but we would need six control lines.

3.1.2 Image Line to Control Line Relationship

Fig. 2(b) illustrates the concept of establishing a relationship between a straight line in the image and its corresponding control line in object space. As indicated earlier, the straight line in image space is the result of a line fitting process, for example by segmenting the raw edge into straight line segments.

There are various ways to formulate a relationship between the fitted line, the control line, and the orientation parameters. *Tommaselli and Lugnani* (1988) suggest to use the following constraint:

$$\lambda \mathbf{R}\mathbf{n}' = \mathbf{n} \tag{3}$$

with λ a scale factor, $\mathbf{R}$ the attitude matrix, $\mathbf{n}'$ the normal of the plane defined by the perspective center C and image line L', and $\mathbf{n}$ the normal of the plane defined by the perspective center C and control line L. Expanding Eq. 3 to components and eliminating the scale factor λ leads to two independent equations. Thus, every line reduces the rank deficiency by two, confirming the fact that three non-collinear lines are necessary to solve the exterior orientation parameters.

3.2 Orientation with Analytical Curves

Analytical curves are a natural extension from the straight line. Considering the research published related to straight lines, using analytical curves received considerably less attention. The computer vision community primarily focused on a subfamily of general 3D curves, namely conic sections.

3.2.1 Image Point to Curve Relationship

We propose a parametric representation of a general 3D curve $\Gamma(t) = [X(t)\ Y(t)\ Z(t), a \leq t \leq b]$. Vector $\Gamma(t)$ describes the locus of points on the space curve as a function of curve parameter t, ranging from a to b. Now, the collinearity equations are modified to express that a measured point in image space corresponds to $\Gamma(t)$. Using homogeneous coordinates we have

$$\begin{bmatrix} x_j \\ y_j \\ 1 \end{bmatrix} = \lambda_j \begin{bmatrix} r_{11} & r_{12} & r_{13} & -(r_{11}X_C + r_{12}Y_C + r_{13}Z_C) \\ r_{21} & r_{22} & r_{23} & -(r_{21}X_C + r_{22}Y_C + r_{23}Z_C) \\ -r_{31}/f & -r_{32}/f & -r_{33}/f & (r_{31}X_C + r_{32}Y_C + r_{33}Z_C)/f \end{bmatrix} \begin{bmatrix} X(t) \\ Y(t) \\ Z(t) \\ 1 \end{bmatrix} \tag{4}$$

Denoting the 3×4 matrix in (4) by $\mathbf{S}$ and eliminating the scalar λ_j yields modified collinearity equations

$$x = \frac{\mathbf{S}_1[X(t)\ Y(t)\ Z(t)]^T}{\mathbf{S}_3[X(t)\ Y(t)\ Z(t)]^T} \quad \text{and} \quad y = \frac{\mathbf{S}_2[X(t)\ Y(t)\ Z(t)]^T}{\mathbf{S}_3[X(t)\ Y(t)\ Z(t)]^T} \tag{5}$$

with $\mathbf{S}_i$ corresponding to the i^{th} row of $\mathbf{S}$. Since the 3D location of object points is uniquely determined by the value of curve parameter t, the image coordinates of object points are now functions of the six camera parameters and the curve parameter t, e.g.

$$x = G_x(X_C, Y_C, Z_C, \omega, \varphi, \kappa, t) \quad \text{and} \quad y = G_y(X_C, Y_C, Z_C, \omega, \varphi, \kappa, t) \tag{6}$$

To arrive at a set of linear equations, (6) must be linearized. Linearization requires initial values for the pose parameters as well as an estimate t_o for the curve parameter.

Every image point renders two equations but increases the number of unknowns by one (curve parameter t). Hence, it contributes only one degree of freedom to the overall redundancy budget. However, there is additional, independent information that can be used. As shown in detail in *Zalmanson* (2000), differential curve information in form of tangent and curvature can be used at the same measured point (x, y), resulting in four equations. This requires a measurement for the tangent direction and the curvature, however.

3.2.2 Image Curve to Control Curve Relationship

There is an explicit relationship between the parameters of conic sections in image and object space, involving the orientation parameters. Conic sections are an interesting family of analytical curves because they are invariant under perspective transformations. That is, a conic curve or section in object space is imaged as a conic. This can be easily explained with basic geometry. Suppose a conic has its origin in the perspective center. The image plane intersects this conic resulting in a conic curve or conic section. The same is true for the plane in object space that contains the conic curve.

Conic curves are usually expressed explicitly by $ax^2 + bxy + cy^2 + dx + ey + f = 0$. This equation can also be written as:

$$\begin{bmatrix} x & y & 1 \end{bmatrix} \begin{bmatrix} a & b/2 & d/2 \\ b/2 & c & e/2 \\ d/2 & e/2 & f \end{bmatrix} \begin{bmatrix} x \\ y \\ 1 \end{bmatrix} = 0 \quad \text{or} \quad \mathbf{XQX}^T = 0 \tag{7}$$

$\mathbf{Q}$ is the conic matrix and contains the conic parameters $a, \ldots, f$. We can use the general conic curve equation (7) to express the conic curves in image and object space. Let $\mathbf{Q}'$ be the conic matrix in image space and $\mathbf{Q}_p$ the corresponding control conic curve represented in a local coordinate system. The principal plane of this local system is identical to the plane that contains the control conic in object space. The following six condition equations exist between the elements of $\mathbf{Q}'$ and $\mathbf{Q}_p$:

$$\begin{array}{lll} k\mathbf{Q}'[1,1] - \mathbf{Q}_p[1,1] = 0 & k\mathbf{Q}'[1,2] - \mathbf{Q}_p[1,2] = 0 & k\mathbf{Q}'[1,3] - \mathbf{Q}_p[1,3] = 0 \\ k\mathbf{Q}'[2,2] - \mathbf{Q}_p[2,2] = 0 & k\mathbf{Q}'[2,3] - \mathbf{Q}_p[2,3] = 0 & k\mathbf{Q}'[3,3] - \mathbf{Q}_p[3,3] = 0 \end{array} \tag{8}$$

As shown in *Zalmanson* (2000), the degree of freedom associated with space curves is directly related to the number of parameters that uniquely define the curve. For conic curves five independent parameters exists. It follows that only five independent equations can be used from Eq. 8. One of the six equations can be used to eliminate the scale factor k. We realize that one control conic is not enough to recover the six exterior orientation parameters.

3.3 Orientation with Free-form Control Curves

As elegant as the use of analytical curves for the pose estimation is, its application is limited because such 3D curves hardly exist in photogrammetry and remote sensing applications. To exploit the full potential of linear and areal features, free-form curves and free-form surfaces must be included in the orientation process. *Besl and McKay* (1992) first introduced free-form shapes for solving the registration problem with curves and surfaces. The authors describe a general-purpose, representation-independent method for registering a variety of 3D shapes such as point sets, free-form curves and surfaces. The iterative closest point (ICP) algorithm is the underpinning for the registration of 3D shapes. It requires only a procedure to find the closest point on a geometric entity to a given point. Subsequently, the ICP approach enjoyed a great deal of interest and success in solving many registration problems. In all these applications, a general weakness of the approach surfaced, however. While it always converges to a minimum value from any given initial transformation parameters, its convergence into a global minimum cannot be guaranteed. Thus, to avoid incorrect transformation parameters, the initial parameter approximations must be quite accurate. Often times, this is a tough requirement as it may necessitate the use of a matching strategy that ultimately yields a set of corresponding point primitives. Over the years, many curve and surface matching strategies have been proposed with recent trends mostly devoted to exploiting differential and semi-differential invariants associated with a variety of 2D and 3D geometric transformations. *Zalmanson* (2000) proposes an alternative approach to circumvent the local minimum problem of the ICP method. The concept of parametric curves allows the simultaneous estimation of the closest point *and* the orientation parameters. This significantly improves the convergence rate compared to classical ICP methods.

A 3D free-form curve, Γ_f, is represented as a sequence of vertices $V = \{V_i\}$. This induces a set of ordered line segments (polyline). As described in the previous section, we then determine the orientation parameters by minimizing the distance between a bundle ray and the polyline.

3.4 Orientation with Control Surfaces

In this section we assume that surfaces are known in object space. The most frequently occurring cases are known planes and free-form surfaces, such as DEMs and DTMs. We approximate free-form surfaces by a set of planar surface patches—in analogy to straight lines and free-form curves. Therefore we only sketch the solution for using planar surfaces as control surfaces.

Obviously, dealing with surfaces requires that surface features extracted from sensors are three-dimensional. An example for a 3D sensor is a range finder. When working with a 2D imaging sensor, 3D surface features are obtained from two or more images. For the following discussion we assume a 3D model space with measured or derived points that are known to be on a planar surface.

3.4.1 Model Point to Control Plane Relationship

The problem of orienting stereomodels to DEMs was first suggested by *Ebner and Strunz* (1988) with a target function that minimizes the $z-$differences. This is not an unbiased estimation of the orientation parameters because it is direction dependent. We propose to use as a target function the distance from a model point to the known surface along the surface normal, instead. Let $\mathbf{q}$ be a point in model space, subjected to a 3D similarity transformation. Then we have $\mathbf{q}' = s\mathbf{R}_a\mathbf{q} - \mathbf{t}$ with s a scale factor, $\mathbf{R}_a$ an orthogonal matrix that rotates the model space into the object space, and $\mathbf{t}$ the translation vector. Further let S be the surface, expressed in the Hessian normal form. Then, the shortest distance d from $\mathbf{q}'$ to surface S, is defined by

$$d = \mathbf{q}' \cdot \mathbf{h} - p \tag{9}$$

with $\mathbf{h} = [\cos\alpha \;\; \cos\beta \;\; \cos\gamma]$ the three directional cosines and p the distance of surface S from the origin. The target function (9) combines the unknown seven orientation parameters with the control surface and the observed model points. Hence it is an ideal starting point to formulate an adjustment procedure for estimating the orientation parameters. For every control plane S_i three independent equations are available. At least three non-parallel control surfaces are required to solve the orientation parameters. For more details on the linearization of Eq. 9 and an analysis of suitable control planes, the interested reader is referred to *Schenk* (1999a).

3.4.2 Model Plane to Control Plane Relationship

The alternative approach to perform the orientation with control surfaces is to fit a surface through all model points that correspond to the control surface. We sketch the procedure for planar surfaces. Let S be a known plane in object space and T a plane in model space, for example fitted through the model points $\mathbf{q}_i$. As a target function we wish to minimize the differences between S and T. The challenge is to find a suitable representation for T in order to allow a similarity transformation.

Suppose a sphere, centered at the origin of the coordinate system with a radius such the plane to be represented becomes a tangent plane. Then planes can be represented by the triplet $\{\varphi, \theta, p\}$ with φ, θ the spherical coordinates of the tangent point, and p the shortest distance of the plane to the origin. Let $\mathbf{R}_a$ be a 3D rotation that operates on the plane in the suggested representation. This will change the direction of the surface normal, expressed by $\mathbf{R}_{\varphi\theta}$ as follows $\mathbf{R}'_{\varphi\theta} = \mathbf{R}_a\mathbf{R}_{\varphi\theta}$. Let us now apply a translation, $\mathbf{t}$, on the plane. It will change all three quantities $\{\varphi, \theta, p\}$. This may come as a surprise because the surface normal does not change its direction under translation. But our representation requires a sphere, centered at the origin, with a radius such that plane S becomes a tangent plane. Translating the plane changes both, the radius and the tangent point (closest point) represented by spherical coordinates. Finally, a scale factor has only an effect on p.

The three elementary transformations can be combined and we arrive at an explicit relationship between $\{\varphi, \theta, p\}$ and its transformed coefficients $\{\varphi', \theta', p'\}$. Now, minimizing the differences between the control plane, expressed by the coefficients $\{\varphi_c, \theta_c, p_c\}$ and the transformed coefficients leads to three condition equations that can be formulated independently for one correspondence model plane to control plane.

There is an interesting twist to the problem of plane to plane transformation in that it can be reduced to the traditional point solution. For this to see imagine that any independent combination of three non-parallel planes leads to a set of intersected points. Repeating the same operation in object space with the corresponding control planes leads to set of intersected points. The two sets of points can now be used for establishing the transformation parameters with a point-based approach.

3.5 Summary

In this section we sketched orientation procedures based on linear and areal control features. This was accomplished by establishing a relationship between orientation parameters, image and control features. The underlying assumption was that the correspondence between image and control features is known, for example by a prior matching process. The goal was to derive a target function that minimizes a distance in object space for an unbiased estimation of the orientation parameters. Whenever possible we formulated a relationship between image (model) points and control features or between image (model) features and control features, respectively. The table below summarizes the most pertinent results.

Table 1: Summary of control features and their use in recovering the exterior orientation parameters.

feature	**point to feature relationship**	**feature to feature relationship**
straight lines	image points to control lines	image line to control line
space curves	image points to control curve	coefficient to coefficient relationship for conic sections
free-form curves	image points to control polylines	not applicable
planar/higher order surfaces	model point to control surface	planar surface to control plane
free-form surfaces	model points to DEM	not applicable

4 Future Challenges

4.1 Tie Features

Classical aerial triangulation, including automatic aerial triangulation, deals with control points and tie points. We strongly suggest to expand this concept to include linear and areal features, that is, to move from points to features. The previous section presented solutions to the problem of using control features instead of control points. This permits the orientation of single images, known as single photo resectioning, but we are still far from a feature-based automatic aerial triangulation because of the lack of suitable models for tie features. What are the problems? Surprisingly, there is virtually no research related to tie features. Consequently, there is long list of exciting future challenges awaiting to be tackled. We briefly comment on a few key issues.

To make a point let us begin with straight lines. Suppose a straight line in object space is imaged in n images, $n > 2$. Suppose further that the orientation of the n images is known. How would you determine the most likely position of this line in object space, assuming that the orientation parameters and the image lines have random errors?

Of paramount interest is an optimal representation of features. An optimal representation should satisfy several criteria, a few of which are listed below (in non-mathematical terms)

- the representation should be unique and should include only independent parameters
- the representation should either avoid singularities or gracefully deal with them
- the representations in image and object space should correspond
- the representation should be amenable to geometric modeling, such as rigid body or 3D similarity transformations
- the representation should be amenable for stochastic modeling

A 3D straight line, for example, has four degrees of freedom. Representing it by two points violates the first criterion because out of the six parameters, two are dependent. Several 4-parameter representations have been proposed. A popular one is to consider a 3D line as the intersection of two planes, one of which is parallel to the $x-$axis, defined by $x = a_1 z + b_1$ and the other one parallel to the $y-$axis, defined by $y = a_2 z + b_2$, see *Ayache and Faugeras* (1989). The 4-tuple $\{a_1, b_1, a_2, b_2\}$ defines the 3D line with a direction vector $[a1\ a_2\ 1]$ and an intersection with the $x, y-$plane of $[b_1\ b_2\ 0]$. This representation has a singularity for lines that are perpendicular to the $z-$axis. Another difficulty is related to the stochastic model: how do we express uncertainties of the line with respect to the four suggested parameters? We realize that the search for an optimal representation of straight lines is not an easy one and by no means as straight-forward as one may suspect at first. The quest for optimal representations of other than straight line features poses an even greater challenge.

4.2 Curve Fitting

As discussed in Sec. 3 there are two different approaches to recover the orientation from control features. The point to feature relationship leads to extended collinearity equations while the second approach usually establishes conditions between image and control features. In the second approach, the extracted image feature must be parameterized—a task that is accomplished by fitting the appropriate analytical feature to the data points. This is not an easy problem for clutter and noise may make it hard to decide which image primitives belong to the curve to be fitted. Moreover, the extracted image curve may be heavily fragmented and the fragments may be poorly distributed.

Apart from the more practical problems there are still theoretical issues, despite the good number of publications dealing with curve fitting. Take the problem with the target function, for example. It is common in the computer vision community to use the algebraic distance of a curve as the entity to be minimized. This approach does not render an unbiased estimation of the curve parameters, however, because it minimizes along a fixed direction. Imagine an ellipse to be fitted through data points. The target function should minimize the distance from the measured points (x, y) to the ellipse along its normal. The algebraic distance $F(x, y)$ is not identical with the normal vector; it is only one component of the vector.

4.3 Multisensor Aerial Triangulation

There is an increasing use of multiple sensors for deriving complementary information. By combining sensors that use different physical principles and record different properties of the object space, complementary and redundant information becomes available. If merged properly, multisensor data may lead to a more stable and consistent scene description. Ideally, proven concepts and methods in remote sensing, digital photogrammetry and computer vision should be combined in a synergistic fashion. Multisensor fusion begins with sensor alignment that involves establishing a common reference frame and determining the pose of all sensors involved.

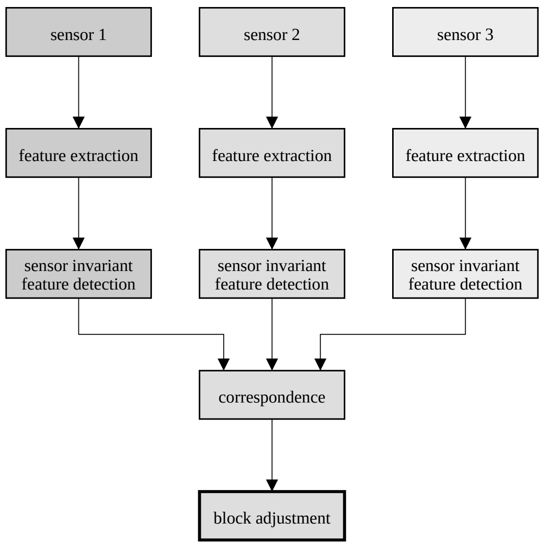

Figure 3: Blockdiagram of multisensor aerial triangulation based on sensor invariant features.

If the sensors are mounted on the same platform, direct orientation is the standard solution to align the sensors. To improve the registration, an aerial triangulation involving multiple sensors is suggested. A useful combination of sensors includes an aerial imaging system, an airborne laser scanning system, and a hyperspectral system. Recently, LIDAR emerged as a new technology for rapidly capturing data of physical surfaces. The high accuracy and automation potential enables a quick delivery of DEMs/DTMs derived from the raw laser data for urban areas. Multispectral and/or hyperspectral data provide further clues about surface properties, such as composition, roughness and slope. The increasing spatial resolution and accuracy, together with the rich information content of hyperspectral image data opens new avenues for automating surface reconstruction and object recognition of urban environments.

Fig. 3 illustrates how the orientation of different sensors can be approached. The proposed method is based on the notion of sensor-invariant features. Such features are caused by the same physical phenomena in object space, see *Schenk and Csathó* (2002) for more details.

5 Concluding Remarks

In this paper we have strongly argued for using linear and areal features in automatic aerial triangulation instead of points. This makes the matching more robust, although more complex to implement. Yet another advantage is the circumstance that the same features can be used in automatic aerial triangulation and in subsequent processes. That is, extracting features and perceptually organize them into higher order structures that may be more meaningful with a view on scene interpretation and object recognition, is only performed once. In general we opt for broadening the fairly narrow focus of automatic aerial triangulation and capture this notion by the following bullet items:

from points to features: see comments above.

integration of automatic aerial triangulation with other photogrammetric procedures: use the same feature extraction, grouping and matching engine in automatic aerial triangulation and other processes. The most appealing example is the combination of automatic aerial triangulation and automatic surface reconstruction.

from single sensor to multi-sensor aerial triangulation: different sensor types, such as frame, panoramic, pushbroom, and whiskbroom types require different sensor modeling.

from aerial triangulation to general sensor orientation: establishing a general sensor orientation framework that would include sensor alignment and image registration, for example.

References

Ayache, N. and O. Faugeras (1989). Maintaining representation of the environment of a mobile robot. *IEEE Trans. on Robotics Automation*, **5**(6), 804–819.

Besl, P. and N. McKay, (1992). A Method for Registration of 3D Shapes. *IEEE Trans. Pattern Analysis and Machine Intelligence*, **14**(2), 239–256.

Ebner, H. and G. Strunz (1988). Combined Point Determination Using Digital Terrain Models as Control Information. In *International Archives of Photogrammetry and Remote Sensing*, **27**(B11/3), 578–587.

Förstner, W. (2000) New Orientation Procedures. In *International Archives of Photogrammetry and Remote Sensing*, **33**(B3/1), 297–304.

Habib, A. and T. Schenk (2001). Accuracy analysis of reconstructed points in object space from direct and indirect exterior orientation methods. In *Heipke, C., Jacobsen, K., Wegmann, H. (Eds.), Integrated Sensor Orientation, OEEPE Publication No. 43.*, 47–52.

Habib, A., A. Asmamaw, D. Kelley and M. May (2000). *Linear features in photogrammetry.* Report No. 450, Department of Civil and Environmental Engineering and Geodetic Science, The Ohio State University, Columbus, OH 43210.

Heipke, C., Jacobsen, K., Wegmann, H. (2002). Analysis of the Results of the OEEPE-Test Integrated Sensor Orientation. In *Heipke, C., Jacobsen, K., Wegmann, H. (Eds.), Integrated Sensor Orientation, OEEPE Publication No. 43.*, 53–72.

Heipke, C. (2002). Photogrammetry & Fernerkundung—vom Elektronenmikroskop bis zur Planetenbeobsachtung. In *Deutsche Geodätische Kommission (Ed.): am Puls von Raum und Zeit*, 54–61.

Jaw, J.J. (1999). *Control Surface in Aerial Triangulation.* PhD dissertation, Department of Civil and Environmental Engineering and Geodetic Science, The Ohio State University, Columbus, OH 43210.

Lee, Y. (2002). *Pose estimation of line cameras using linear features*. PhD dissertation, Department of Civil and Environmental Engineering and Geodetic Science, OSU, 162 p.

Schenk, T. (1999). *Matching Surfaces*. Technical Notes in Photogrammetry, No. 15, Department of Civil and Environmental Engineering and Geodetic Science, The Ohio State University, Columbus, OH 43210, 21 pages.

Schenk, T. and B. Csathó (2002). Fusion of LIDAR data and aerial imagery for a more complete surface description. In *International Archives of Photogrammetry and Remote Sensing*, **34**(3A), 310–317.

Schenk, T. (2002). Towards a feature-Based Photogrammetry. *Bildteknik/Image Science*,**2002**(1), Swedish Society for Photogrammetry and Remote Sensing, Stockholm.

Schenk, T. (1999b). *Digital Photogrammetry*. TerraScience, Laurelville, OH 43135, 428 pages.

Tommaselli, A. and J. Lugnani (1988). An alternative mathematical model to collinearity equations using straight features. In *International Archives of Photogrammetry and Remote Sensing*, **27**(B3), 765–774.

Zalmanson, G. (2000). *Hierarchical Recovery of Exterior Orientation from Parametric and Natural 3D Curves*. PhD dissertation, Department of Civil and Environmental Engineering and Geodetic Science, OSU, 121 p.